JGR Atmospheres

RESEARCH ARTICLE
10.1029/2024JD042827

Do Microplastics Contribute to the Total Number Concentration of Ice Nucleating Particles?

Daria Tatsii[1], Blaž Gasparini[1], Ioanna Evangelou[1], Silvia Bucci[1], and Andreas Stohl[1]

[1]Department of Meteorology and Geophysics, University of Vienna, Vienna, Austria

Key Points:

- We assess road traffic-related microplastic number concentrations in the atmosphere and their contribution to total ice nucleating particles
- Microplastics can disperse throughout the entire troposphere and reach regions with low natural ice nucleating particle concentrations
- Contribution of ice-active microplastics can be relatively large in certain regions in mixed-phase and cirrus clouds

Supporting Information:

Supporting Information may be found in the online version of this article.

Correspondence to:

D. Tatsii,
daria.tatsii@univie.ac.at

Citation:

Tatsii, D., Gasparini, B., Evangelou, I., Bucci, S., & Stohl, A. (2025). Do microplastics contribute to the total number concentration of ice nucleating particles? *Journal of Geophysical Research: Atmospheres*, *130*, e2024JD042827. https://doi.org/10.1029/2024JD042827

Received 28 OCT 2024
Accepted 10 JAN 2025

Author Contributions:

Conceptualization: Daria Tatsii, Blaž Gasparini, Andreas Stohl
Formal analysis: Daria Tatsii, Ioanna Evangelou
Investigation: Daria Tatsii
Methodology: Daria Tatsii, Blaž Gasparini
Supervision: Silvia Bucci, Andreas Stohl
Visualization: Daria Tatsii
Writing – original draft: Daria Tatsii
Writing – review & editing: Daria Tatsii, Blaž Gasparini, Ioanna Evangelou, Silvia Bucci, Andreas Stohl

Abstract Microplastics (MPs) can be transported into clouds, where they may act as ice nucleating particles (INPs). However, MPs have not been considered as contributors to INP concentrations. Here, we quantify road traffic-related MP number concentrations, and estimate their contribution to total INP concentrations using the atmospheric transport model FLEXPART. We find that under a high emission scenario ice-active MPs can account from about 0.1% to more than 40% of the total INP number in immersion freezing conditions in the tropics, whereas for cirrus conditions, their contribution can be up to about 7% over the tropical Pacific and up to about 20% over East Antarctica. Thus, in regions where other effective INPs are rare, ice-active MP concentrations may be sufficient to trigger heterogeneous nucleation of ice crystals in mixed-phase clouds or cirrus. This suggests that MP may affect cloud formation and highlights the need to reduce uncertainty in MP emissions and their fate in the atmosphere as plastic use continues to grow.

Plain Language Summary Microplastics are tiny plastic particles that can travel long distances through the air and reach remote regions. However, microplastics have been overlooked in studies of cloud ice formation, which is induced by so-called ice nuclei—particles that help to form ice crystals. This model study explores how many microplastic particles from road traffic are in the atmosphere and how much they contribute to ice nuclei concentrations compared to other particle types, such as dust or sea spray. We find that microplastics can account for up to 40% of all ice nuclei under certain freezing conditions. Thus, microplastics may trigger ice crystal formation in clouds, thereby affecting cloud properties, which are important for the global climate. As plastic production and usage is expected to increase, further research into microplastics' impact on the atmosphere is crucial.

1. Introduction

Microplastics (MPs), defined as synthetic organic polymers ranging in size from 1 μ m to 5 mm (Hale et al., 2020), have been documented in various environmental compartments including oceans, soils, and the atmosphere (Ahmed et al., 2022). Due to their relatively low density, small size, and often complex shape, MPs can be transported over long distances within the atmosphere (S. Allen et al., 2019; Kau et al., 2024) and reach the upper troposphere (Bucci et al., 2024). In the atmosphere, MPs are exposed to UV radiation and oxidants such as ozone, which can cause changes in their morphology such as surface roughening, formation of pores, and increased specific surface area, and make MPs more hydrophilic (Jiang et al., 2023). Hygroscopicity can also be increased by biofilm coatings (Teska et al., 2024). These factors can activate MPs as cloud condensation nuclei (CCNs) or ice nucleating particles (INPs), affecting cloud formation and the size distribution of cloud droplets and ice crystals, with possible consequences for the Earth's radiation budget and climate (Aeschlimann et al., 2022).

Estimating the impact of MPs on clouds remains a challenge (Aeschlimann et al., 2022). Nevertheless, in recent years, interest in MPs as potential INPs has been growing. Wang et al. (2023) and Xu et al. (2024) documented the presence of MPs in cloud water. Ganguly and Ariya (2019) found that polymers such as polyethylene (PE) and polypropylene (PP) can indeed act as INPs. More recently, Seifried et al. (2024) and Busse et al. (2024) demonstrated that PE, PP, polyethylene terephthalate (PET), polyvinyl chloride (PVC), and low density polyethylene (LDPE) can heterogeneously nucleate ice in the immersion freezing mode, the dominant freezing pathway in the mixed-phase cloud regime (Murray et al., 2012). According to Seifried et al. (2024), the number of ice nucleation sites per surface area of PE, PP, and PET is similar to those of fungal spores and volcanic ash. These findings suggest that it is important to investigate the role of MPs as potential INPs in the atmosphere. Mixed-phase and cirrus clouds play a critical role in the climate system affecting precipitation formation, the energy

balance of the Earth, and its response to global warming (Gasparini & Lohmann, 2016; Gasparini et al., 2023; Korolev et al., 2017; Matus & L'Ecuyer, 2017; Murray et al., 2021; Tan et al., 2016).

In this study, we simulate the atmospheric transport of particles from the largest primary source of MPs, which are emissions related to road traffic. This includes tire wear particles (TWPs), brake wear particles (BWPs), particles from road markings or painted coatings on the road surfaces (RMPs), and from polymer-modified bitumen (PMBPs). We focus on these sources because they are relatively well known compared to other MP sources, for which emission estimates often deviate by orders of magnitude. Polymers are widely incorporated as additives in tires, road markings, and bitumen to enhance their resistance to the fluctuations of temperature or humidity, and UV degradation (Vogelsang et al., 2018). Mechanical abrasion caused by friction between the moving tire and the road surface leads to the wear of tires, road markings, and asphalt. Similarly, BWPs are released due to the friction between brake linings and rotating components.

Despite their recognized presence in the atmosphere (Harrison et al., 2012; Morioka et al., 2023; Myszka et al., 2023), road traffic-related MPs have never been considered as important contributors to the total INP concentrations on the global scale, even though road dust in general does contribute to INPs in urban areas (Chen et al., 2024). Therefore, the aim of this study is to quantify road traffic-related MP number concentrations and their potential contribution to the total INP number concentrations based on atmospheric transport model simulations.

2. Materials and Methods

We follow a five-step procedure to obtain MP number concentrations: (a) estimation of road traffic-related MP emissions from wear of tires, brakes, road markings, and polymer modified bitumen; (b) development of size distribution scenarios and estimation of airborne fractions for each size; (c) simulation of the atmospheric transport of MPs using a Lagrangian particle dispersion model; (d) estimation of the fraction of MPs that act as INPs; and (e) comparison of the obtained values with existing estimates of total INP number concentrations in mixed-phase and cirrus clouds.

2.1. Emissions of Road Traffic-Related MPs

According to Kole et al. (2017), annual emissions of TWPs are 0.81 kg per person, which is equivalent to a global total of 6,350 kt/year, based on a global population of 7.84 billion in 2020. We assume that 50% (3,175 kt/year) of these emissions are MPs, since typically 30% of the tire mass is styrene-butadiene rubber and 20% is butadiene rubber (Grigoratos & Martini, 2014). Following the results of Evangeliou et al. (2020), which are based on GAINS (Greenhouse gas-Air pollution Interactions and Synergies) model output (Amann et al., 2011), global emissions of BWPs are 175 kt/year. Based on Burghardt and Pashkevich (2023) and Enfrin et al. (2022), the median global emission of MPs from road markings is 0.063 kg per person per year, which corresponds to a total of 494 kt/year worldwide. According to the estimates of Pyshyev et al. (2016), 11,093 kt/yr polymer-modified bitumen is used worldwide for road surfaces. About 5% of weight are polymers, that is, at most 555 kt/year MPs could be emitted into the environment.

2.2. Airborne Fractions and Size Distribution of MPs

Adding the contributions from all road traffic-related sources, the global total MP emission into the environment is 4,399 kt/year. However, only a fraction of this total emission enters the atmosphere. For each MP source, the emissions were therefore weighted by their assumed airborne fractions (Table 1). These fractions are subjects to significant uncertainties due to multiple influencing factors such as vehicle type and speed, tire type, road surface type, weather conditions, and the use of road salt or sand in winter (Evangeliou et al., 2020; Hussein et al., 2008). In this study, we adopt the approach of Evangeliou et al. (2020), who provided estimates for the airborne fractions of MPs smaller than 10 μ m (PM10 and PM2.5) from TWPs and BWPs. We use their lower and upper bounds for each size mode and emission type as our lower and upper case scenarios (Table 1). According to Kreider et al. (2010) and Broeke et al. (2008), PM10 emissions from RMPs account for 4% of the total emissions, whereas PM2.5 accounts for 1%. For PMBPs, the PM10 fraction is 35%, whereas PM2.5 is 10% (Snilsberg et al., 2008). We use these reported airborne fractions for RMPs and PMBPs as both the lower and upper bounds. Throughout this study, we will refer to the minimum airborne MP fraction scenario as MIN and to the maximum airborne MP fraction scenario as MAX.

Table 1
Scenarios of MP Airborne Fractions for Each Emission Type: TWPs, BWPs, RMPs, and PMBPs

	Airborne fraction scenario, %			
	MIN		MAX	
Emission type	PM2.5	PM10	PM2.5	PM10
Tire Wear Particles (TWPs)	0.25	2.5	4	40
Brake Wear Particles (BWPs)	30.00	60.0	70	100
Road Marking Particles (RMPs)	1.00	4.0	1	4
Polymer Modified Bitumen Particles (PMBPs)	10.00	35.0	10	35

Note. The MIN and MAX scenarios for TWPs and BWPs are similar to the airborne fraction scenarios proposed by Evangeliou et al. (2020). Details on the fractions for RMPs and PMBPs can be found in Section 2.2.

As noted by Evangeliou et al. (2020), the size distribution within the PM10 and PM2.5 modes of road traffic-related MPs are highly uncertain. We follow several studies that provide various scenarios for TWPs and BWPs (Evangeliou et al., 2020), road marking particles (Broeke et al., 2008; Kreider et al., 2010), and asphalt particles (Snilsberg et al., 2008). The scenarios are shown in Figures 1a–1d. Similar to Evangeliou et al. (2020), for our model simulations, we discretize the particle size distribution into six size classes, where the PM2.5 mode is represented by three size classes with volume equivalent diameters, d_{eq}, of 0.5, 1.0, 2.1 μm; and the PM10 mode by six size classes with d_{eq} of 0.5, 1.0, 2.1, 3.2, 6.0, and 9.5 μm. Note that size distributions are expressed in terms of relative mass contribution of each size bin to total PM10. For TWPs and BWPs, the contributions are referenced to the total PM10 emissions, which is considered representative of the airborne fraction of TWP and BWP emissions (Evangeliou et al., 2020). A similar approach was applied to RMPs and PMBPs.

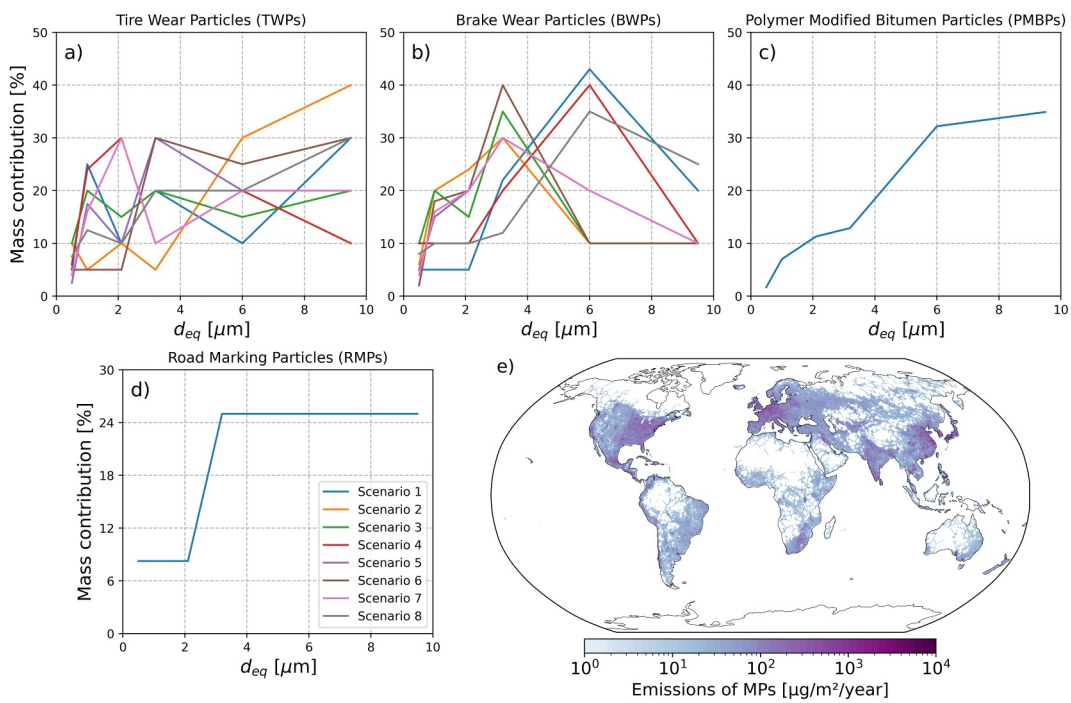

Figure 1. Size distribution scenarios of TWPs, BWPs, RMPs, and PMBPs (a–d) and global map of total MP emissions from road traffic using road lengths as a proxy (e). Size distributions are expressed in terms of mass contribution per size and represented by colored lines. Panels (a and b) have been reproduced from Evangeliou et al. (2020). Panels (c) and (d) show the size distribution of PMBPs and RMPs, based on the studies of Snilsberg et al. (2008), and Kreider et al. (2010); Broeke et al. (2008), respectively.

Our resulting estimates of the atmospheric emissions of road traffic-related MPs are expressed as averages over the size distribution scenarios ($\bar{x}$) ± standard deviation (σ): 259 ± 9 kt/year ($1.0 \cdot 10^{23}$ ± $1.8 \cdot 10^{22}$ particles/year) for the MIN scenario and 1005 ± 139 kt/year ($3.2 \cdot 10^{23}$ ± $5.6 \cdot 10^{22}$ particles/year) for the MAX scenario. These results are between the lower and the higher bound of estimates of D. Allen et al. (2022), who report deposition of atmospheric MPs into the marine environment ranging from 13 to 25,000 kt/year.

To place our total MP emissions in context, it is useful to compare our estimates with global emissions of mineral dust, which is considered the most important source of INPs (Froyd et al., 2022; Murray et al., 2012; Seinfeld et al., 2016). According to Evangelou et al. (2024), annual mineral dust emissions in 2018 were approximately 2,200 Mt/year, corresponding to $1.1 \cdot 10^{26}$ particles/year in PM10 mode, which is three orders of magnitude larger compared to global road traffic-related MPs. Although this would suggest that MPs are a minor contributor to atmospheric INP concentrations, one has to bear in mind that the size distribution of mineral dust particles is shifted to a coarser mode compared to MPs, their density is much higher and their aspect ratios are generally lower than those of MP particles (Abbasi et al., 2023). For example, the modeling study of Evangelou et al. (2024) reveals that the global residence time of resuspended spherical MPs is about 6 days, whereas for resuspended MP fibers, it extends to about 9 days. In contrast, the mean global residence time of mineral dust in the atmosphere is estimated to range between 2 and 6 days (Checa-Garcia et al., 2021; Groot Zwaaftink et al., 2016; Tegen et al., 2019). All these factors lead to shorter atmospheric lifetimes of mineral dust particles compared to MPs and need to be considered for a meaningful comparison. Furthermore, the geographical distribution of emissions of MPs and mineral dust differs substantially. MPs from road traffic are predominantly emitted in or near populated areas (as in our modeled emissions, see Figure 1e), whereas mineral dust mainly originates from the sparsely populated regions with bare soils.

We assume that all MP particles are fragments with an aspect ratio (AR) of 3, which is an average value based on several measurement studies (Järlskog et al., 2022; Kovochich et al., 2021; Sommer et al., 2018; Wilkinson et al., 2023). Following Evangeliou et al. (2020), the density of the simulated particles is set to 1234 kg/m^3. In a final step, the global MP emissions were spatially disaggregated using the paved road length data from the GRIP4 global road database as a proxy (Meijer et al., 2018) (Figure 1e).

2.3. Simulations of Atmospheric Transport

We performed atmospheric transport simulations using a modified version of the Lagrangian dispersion model FLEXPART version 11 (Bakels et al., 2024b) based on hourly ERA5 global meteorological re-analysis data (Hersbach et al., 2020) with 137 vertical levels and a grid resolution of 0.5° × 0.5°. The model simulates the global transport, turbulent diffusion, convection, as well as dry and wet deposition of particles. For the calculation of the particles' trajectories, FLEXPART uses the mean winds from the meteorological input data, parameterized stochastic turbulent motions in the atmospheric boundary layer, and a stochastic convection scheme. Gravitational settling velocities are added to the vertical air velocities to transport the particles (Tatsii, Bucci, et al., 2024a).

We performed a continuous release of 25 million particles per size class, each carrying the same fraction of the globally emitted mass, and with release locations distributed according to our road network proxy (Figure 1e). Their atmospheric transport and deposition was simulated for 2.5 years (from July 2014 to December 2016), of which the first six months were considered as model spin-up and discarded. The result of the simulations is a monthly averaged 3D field of MP mass concentration (M_{conc}). Number concentrations (N_{conc}) were obtained using the following formula: $N_{conc} = M_{conc}/(\rho \cdot V_p)$, where ρ is the particle density and V_p the volume of a particle in the size bin.

According to Aeschlimann et al. (2022), UV aging can alter the hydrophobicity of airborne MPs. In the wet scavenging scheme, their CCN and INP efficiencies were set to values of 0.5 and 0.8, respectively, to be representative of relatively hydrophilic particles (Evangeliou et al., 2020). It is important to note that the exact scavenging efficiencies of MPs are not known. To address this uncertainty, we conducted a sensitivity test where we reduced the scavenging efficiencies (0.25 for CCN efficiency and 0.4 for INP efficiency).

2.4. Ice-Active MP Fraction and Comparison to Total INP Concentrations

For determining the ice-active fraction of MPs, we distinguish two different regimes: mixed-phase clouds where immersion freezing is the dominant freezing mode, and cirrus clouds for which also deposition nucleation is

important. We determine the fraction of spherical particles that can trigger immersion freezing (fr) as a function of air temperature (T) in the range from −18°C to −28°C based on the empirical data for PET provided in Figure 2b in Seifried et al. (2024):

$$fr = 0.0159 \cdot T^2 + 0.6284 \cdot T + 6.2157 \quad (1)$$

We use empirical data on the frozen fractions of spherical PET particles as representative of other polymers such as PP and PE. Seifried et al. (2024) show that aged or non-aged PET, PP, and PE with uniform shapes exhibit similar ice nucleation efficiencies. Consistent results were reported by Busse et al. (2024), who observed similar ice nucleation efficiencies for non-aged PP, PET, and LDPE. The fitted relationship (goodness-of-fit: $R^2 = 0.97$) was then applied to mask and weight the number concentrations of ice-active particles within the specified temperature range (−18°C to −28°C). Within the temperature range of −28°C to −38°C, all particles are considered ice-active. We then compare the MP-derived INP concentrations with the total (dust and marine-sourced) INP concentrations that can trigger immersion freezing as modeled by Herbert et al. (2025). Their results are in good agreement with measured INP concentrations and align well with another modeling study (Chatziparaschos et al., 2023).

MPs are also thought to be able to trigger ice nucleation under cirrus conditions, either through deposition nucleation or immersion freezing of coated MP particles (Aeschlimann et al., 2022). However, the potential of MPs to initiate ice nucleation under cirrus conditions (i.e., at temperatures colder than the homogeneous freezing temperature of water) is still unknown. To cover the range of plausible ice-active fractions of MPs, we propose three possible ice-active fractions (fr) for MP particles in cirrus clouds: 0.001, 0.01, and 0.1. The fractions were chosen based on the assumption that MPs are, on average, less effective INPs compared to certain types of dust. We neglect the dependence of MP ice nucleation on RH_{ice}, which is relevant for cirrus conditions only, as there are no studies looking into it.

We compare the obtained MP INP concentrations at cirrus conditions with the total mineral dust INP number concentrations as modeled by Beer et al. (2022). Note that Beer et al. (2022) do not provide data for marine-sourced INP number concentrations. Their estimates are consistent with previous modeling studies (Gasparini & Lohmann, 2016; Hendricks et al., 2011; Kuebbeler et al., 2014). We neglect other possible INP sources from their study due to their low concentrations or small ice-active fractions, and large uncertainties. For consistency with Beer et al. (2022), we adopt their definition of cirrus clouds, characterized by temperatures colder than 238 K and ice water content greater than 0.5 mg/kg, within pressure levels ranging from the surface to 10 hPa. Temperature and specific cloud ice water content fields were retrieved from the ERA5 meteorological reanalysis (Hersbach et al., 2020).

We also compare our results with the mineral dust number concentrations in cirrus cloud conditions measured during the Atmospheric Tomography Mission (ATom) (Wofsy et al., 2018) and reported in Figure 5c (black circles) of Froyd et al. (2022). Their reported values are spatial averages across five latitudinal ranges from approximately 86°S to 82°N and in cirrus-forming regions (T < 235 K and below the cold point tropopause). We limit our comparison to simulated MP particle size bins of 0.5, 1.0, 2.1, and 3.2 μm, since the airborne Particle Analysis By Laser Mass Spectrometry (PALMS) instrument (Thomson et al., 2000), used to measure mineral dust during the campaigns, covers only the size range from 0.1 μm to 5.0 μm in diameter.

3. Results

We first present the spatial distribution of simulated road traffic-related MPs, followed by their INP number concentrations and estimates of the MP contribution to the total INP number concentration. The "total" INP concentration refers to the sum of mineral dust, marine-sourced, and MP INPs for mixed-phase clouds, and the sum of mineral dust and MP INPs for cirrus clouds. Regions of the globe, for which we report the spatial averages, are shown in Figure S1 in Supporting Information S1.

Simulated seasonal means of MP number concentration as a function of latitude and height are illustrated in Figure 2. MPs are dispersed throughout the troposphere and can reach high altitudes, such as the tropical tropopause, as well as remote regions, including those near the Poles (Figure 2). The highest concentrations are associated with the highest road traffic density—and thus the bulk of MP emissions (Figure 1e)—and are found in

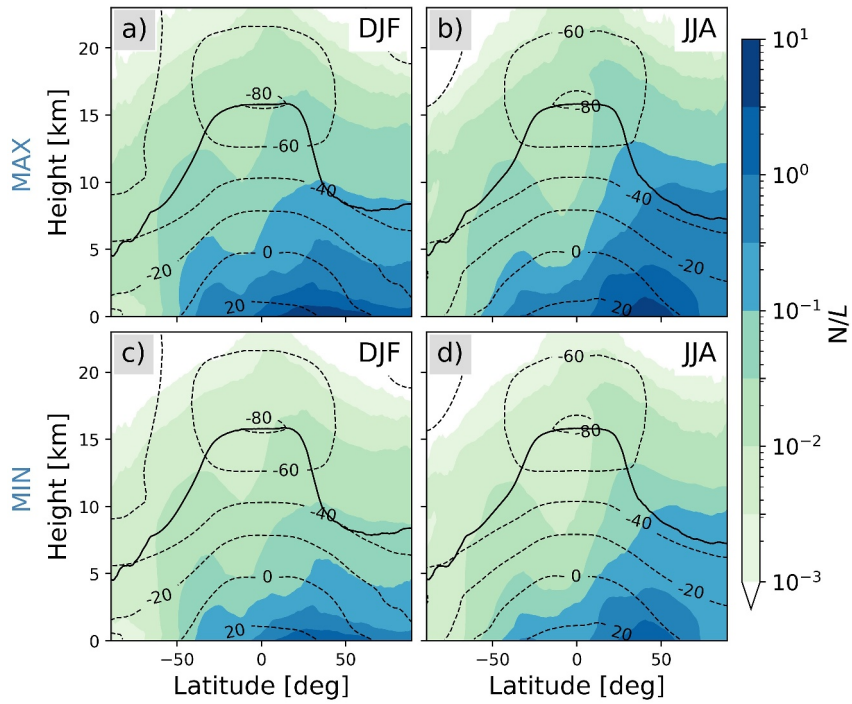

Figure 2. Seasonal mean number concentrations of road traffic-related MPs as a function of latitude and height, expressed in N/L (particles per liter). Panels (a and b) and (c and d) show results for the MAX and MIN scenario, respectively, in each case averaged over all scenarios of the emitted size distribution (Figures 1a–1d). Values are shown for December-January-February (DJF; panels a and c) and June-July-August (JJA; panels b and d). The solid black line shows the climatological mean thermal tropopause, black dashed lines are climatological mean isotherms.

the Northern Hemisphere (NH). Number concentrations $>1/L$ extend up to approximately 2 km in altitude in the NH during DJF (December-January-February) and up to approximately 4 km in JJA (June-July-August) under the MAX scenario (Figures 2a and 2b). This pattern is consistent with deep convection during NH summer, particularly over East Asia and southern North America (Figure 3), transporting MP particles to T<-20°C, where they can affect ice nucleation (see Section 2.4) (Figures 2a and 2b). The Southern Hemisphere (SH), characterized by less road traffic, exhibits lower concentrations. In tropical regions (30°S–30°N), within the layer from about 10 km (−38°C) to the tropical tropopause, where cirrus clouds form frequently, the maximum observed concentration is 0.1/L under the MAX scenario, with concentrations an order of magnitude lower in the MIN scenario (Figure 2). When scavenging efficiencies are reduced by 50%, MP number concentrations generally increase (Figure S2 in Supporting Information S1). For instance, under the MAX scenario, concentrations exceeding 1/L extend up to 4 km in altitude in the NH during DJF and reach the tropopause level during JJA (Figures S2a and S2b in Supporting Information S1).

3.1. Relevance to Mixed-Phase Clouds

Clouds containing varying amounts of liquid or ice mass frequently populate such regions as the Southern Ocean and the Arctic (Korolev et al., 2017), exerting a particularly important control on high latitude climate. Moreover, remote oceanic regions at high latitudes contain low burdens of natural INPs (Herbert et al., 2025). In particular, cloud properties above the Southern Ocean were shown to be very sensitive to INP concentrations; a failure to represent these correctly leads to substantial radiative biases in climate models (Vergara-Temprado et al., 2018).

Figures 3c–3d and 3g–3h and Figures S3c–S3d, S3g–S3h in Supporting Information S1 illustrate the geographical distribution of MP particles at pressure levels between 900 and 600 hPa, which are relevant for mixed-phase cloud formation. As we can see, the MP concentrations are relatively high over NH with spatial mean concentrations of approximately 3/L (0.8/L) at 900 hPa and approximately 1/L (0.3/L) at 700 hPa in the case of MAX (MIN) scenario (Figures 3c–3d and 3g–3h).

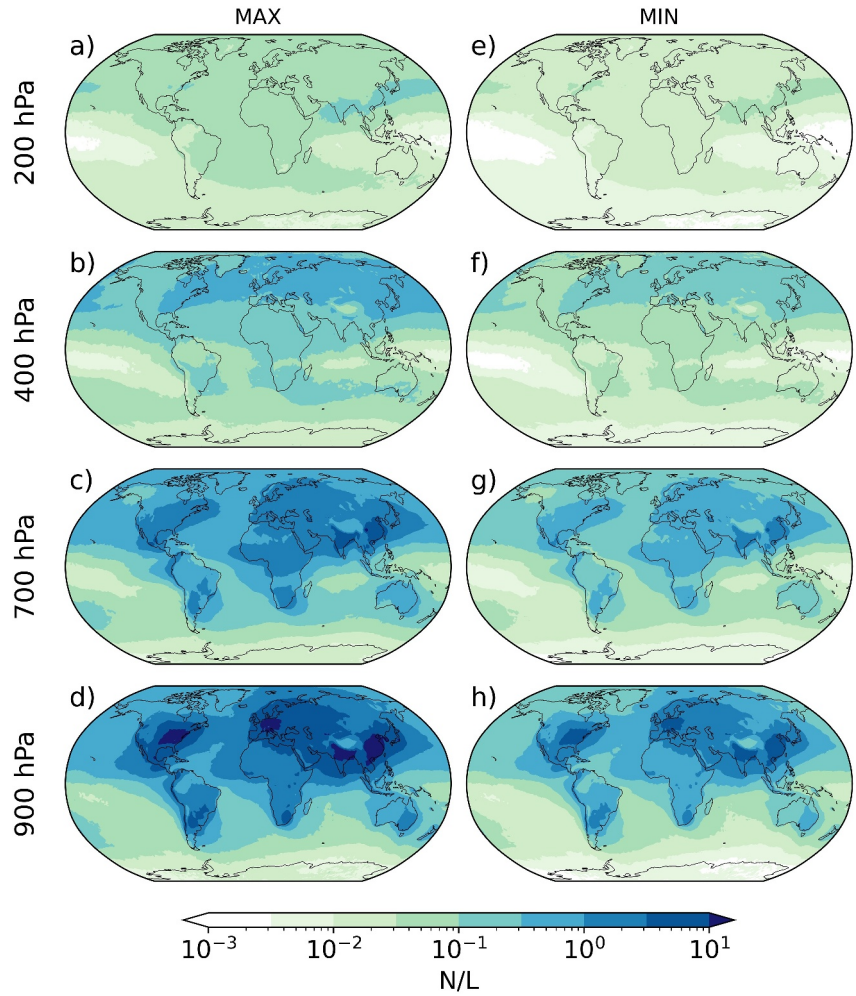

Figure 3. Annual mean number concentrations of traffic-related MPs at different pressure levels, expressed in N/L (particles per liter). Shown is the average over all scenarios for the emitted size distribution (Figure 1e). Left (a–d) and right (e–h) panels show MAX and MIN scenarios, respectively. Panels (a and e) indicate number concentrations at approximately 200 hPa; (b and f) at 400 hPa; (c and g) at 700 hPa; (d and h) at 900 hPa.

In regions of low dust and thus very low natural INPs such as over the Southern Ocean and the Arctic (Herbert et al., 2025; Kanji et al., 2017), already small concentrations (<0.1/L) of INPs could initiate the freezing of cloud droplets (Vergara-Temprado et al., 2018). At 900 hPa, the average MP number concentrations over the Southern Ocean and the Arctic are about 0.05/L and 1.5/L, respectively, in the MAX scenario and 0.01/L and 0.4/L, respectively, in the MIN scenario. At 700 hPa, the concentrations in these regions are slightly lower, 0.05/L and 0.7/L, respectively, in the MAX scenario and about 0.01/L and 0.2/L, respectively, in the MIN scenario.

In the following, we compare MP INP number concentrations under mixed-phase cloud conditions (at temperatures between 0°C and −38°C) with the modeled estimates of mineral dust and marine-sourced INP concentrations from Herbert et al. (2025). In regions such as the Southern Ocean and the Arctic, the mean relative contribution of MPs to the total (mineral dust, marine-sourced aerosols, and MP) INP concentration in the MAX scenario is about 0.2% and 0.7%, respectively, and about 0.06% and 0.2%, respectively, in the MIN scenario (Figures 4c and 4d). The relative contribution of MP to INPs is particularly large in areas of tropical convection (15°S–15°N), which are populated by anvil clouds, the most frequent and radiatively important cloud type in the tropics (Berry & Mace, 2014; Hartmann & Berry, 2017). Even small changes to anvil cloud properties, for example, due to increased rate of heterogeneous drop freezing in convective updrafts or in aged anvil clouds can lead to substantial changes in radiative budgets (Hawker et al., 2021), highlighting the importance of INPs in such regions. Our estimates indicate that in the MAX (MIN) case MPs contribute on average 7% and up to 16% (on average 2% and up to 6%) of the total

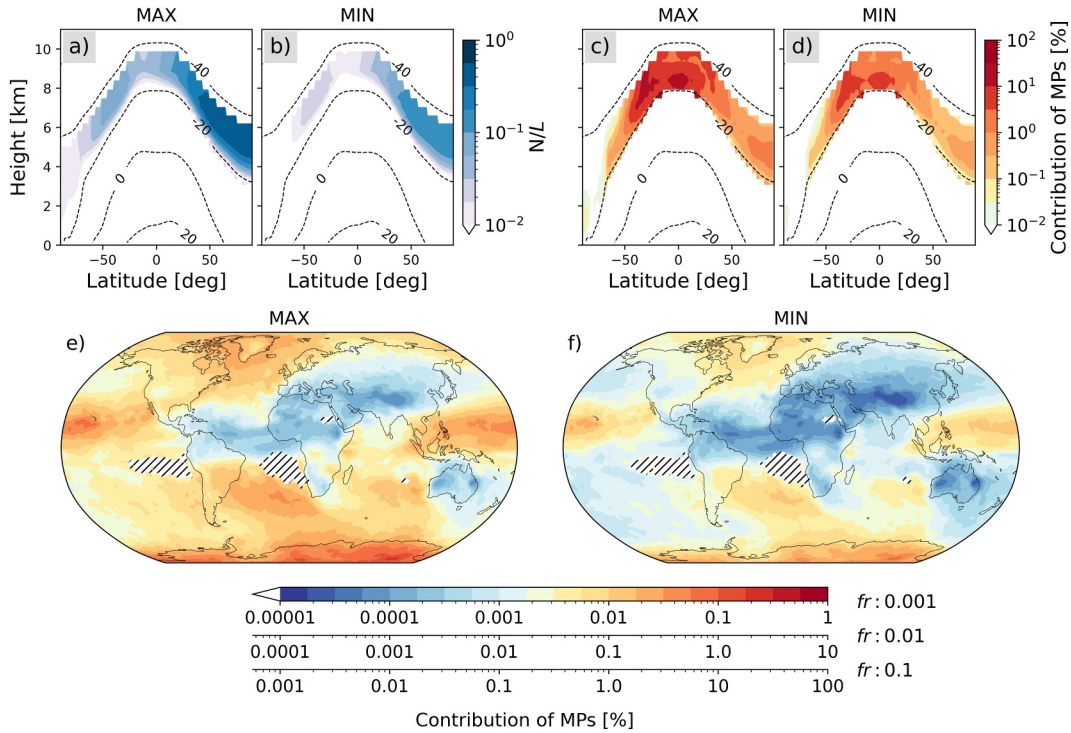

Figure 4. Annual mean of microplastic INP number concentration (a and b) and contribution of the road traffic-related MPs to the total number concentration of INPs in mixed-phase regime as modeled by Herbert et al. (2025) (c and d) and in cirrus cloud conditions as modeled by Beer et al. (2022) (e and f). Number concentration is expressed in N/L (particles per liter). Shown is the average over all size distribution scenarios (Figures 1a–1d). Panels (a, c, and e) and panels (b, d, and f) show MAX and MIN scenarios, respectively. Black dashed lines are climatological mean isotherms. The three colorbar tick labels under panels (e and f) represent the value ranges when assuming different fractions of cirrus-active INPs from MPs (fr), corresponding to 0.001, 0.01, and 0.1 (see Text S1 in Supporting Information S1 for details). No cirrus clouds are present in hatched areas.

(mineral dust, marine-sourced aerosol and MP) INP concentration at those conditions. In the region of 30°S–30°N, the average relative contribution of MPs is 7% and 2% under the MAX and MIN scenarios, respectively, but can locally reach values of up to 41% and 19% (Figures 4c and 4d).

3.2. Relevance to Cirrus Clouds

Figures 3a–3b and 3e–3f and Figures S3a–S3b and S3e–S3f in Supporting Information S1 show the annual mean MP number concentrations at 100, 200, 300, and 400 hPa, pressure levels where cirrus clouds typically form. The highest concentrations are found in the Northern Hemisphere, especially over the North Atlantic, southern North America, and East Asia. For tropical cirrus cloud formation, the focus is on the 100 and 200 hPa levels. Although deep convection transports ice crystals that freeze under mixed-phase conditions or through homogeneous drop freezing up to the tropopause (Bolot & Fueglistaler, 2021), ice nucleation is the dominant mode of cirrus formation in the tropical tropopause layer, above the level of mean convective outflow (Jensen et al., 2013, 2017). Here, average MP concentrations are about 0.05/L in the MAX scenario, and about 0.01/L in the MIN scenario (Figure 3a). Concentrations vary across regions with the largest occurrence of cirrus clouds, such as the Pacific Ocean (0°–30°N), Central Africa, and South East Asia (Gasparini et al., 2023; Sassen et al., 2008). For example, under the MAX scenario, concentrations over these regions reach approximately 0.1/L (Figure 3a). Under the MIN scenario, concentrations in these regions are even smaller. At 400 hPa, the average concentrations in mid latitudes range from about 0.3/L in NH to about 0.1/L in the SH in the MAX scenario and from about 0.1/L to 0.02/L in the MIN scenario (Figures 3b and 3f).

Figures 4e and 4f compares the contribution of road traffic-related MPs to the mineral dust INP number concentration in cirrus clouds of Beer et al. (2022). In the MAX scenario, MPs account for an average relative

Table 2
Comparison of the MP Number Concentrations With the Number Concentrations of Mineral Dust in Cirrus Cloud-Forming Regions (Froyd et al., 2022) Measured During the ATom Campaign (Wofsy et al., 2018)

	This study (MPs), (N/L)		
Latitude range	MIN	MAX	ATom (dust), (N/L)
−80° to −60°	0.006	0.02	~6
−60° to −27°	0.01	0.04	~6
−27° to 27°	0.02	0.05	~5
27° to 60°	0.05	0.14	~70
60° to 80°	0.05	0.16	~80

Note. Only simulated particles with d_{eq} = 0.5, 1.0, 2.1, 3.2 μm are considered, to be consistent with the measured size range.

contribution of approximately 1%, with a maximum of about 7% over the tropical Pacific and an average relative contribution of approximately 6%, with a maximum of about 20% over the East Antarctic, when assuming the ice-active fraction of MPs to be 0.1 (Figure 4e). However, the importance of MPs is negligible in regions with large burdens of mineral dust, such as Africa, northern South America, and the Tibetan plateau. In the MIN scenario, the average relative contribution is approximately 0.4% and 2% with the highest contribution of about 3% and 7% over the tropical Pacific and East Antarctic, respectively (Figure 4f). With ice-active fractions of 0.01 and 0.001, contributions decrease by one and two orders of magnitude, respectively (Figure 4).

We also compared our MP number concentrations with the mineral dust number concentrations measured during the ATom campaigns (Wofsy et al., 2018) in cirrus cloud-forming regions (Table 2). Our simulated MP concentrations in all regions are approximately two orders of magnitude lower than the measured mineral dust concentrations. However, given the large spatial and temporal variability in both measured and modeled dust number concentrations, differences can be substantially smaller in individual air masses.

4. Discussion and Conclusions

In this study, for the first time, we estimate the number concentrations of road traffic-related MPs throughout the troposphere and investigate whether these concentrations are high enough to affect cloud formation. To do this, we performed simulations of the atmospheric transport of MP particles emitted by road traffic under two scenarios. We found that MPs are dispersed throughout the troposphere and can reach regions with low concentrations of natural ice-nucleating particles. Due to their smaller size, lower density and usually greater aspect ratios, MP particles may be more efficiently transported to higher altitudes and remote regions compared to mineral dust.

In immersion freezing conditions, the contribution of MPs can account for 7% on average and exceed 40% of the total (mineral dust, marine-sourced aerosol, and MPs) INP number concentration in parts of the tropics in the MAX scenario. In this scenario, simulated MP number concentrations can reach up to 0.1/L in the tropics above 10 km, whereas in the MIN scenario, concentrations are an order of magnitude lower. Furthermore, under cirrus cloud conditions, the contribution of MPs can be as high as 7%, with an average value of about 1% in the tropical Pacific and as high as 20%, with an average value of about 6% in East Antarctic for the MAX scenario. These findings suggest that in certain regions, MP concentrations may be sufficient to induce heterogeneous nucleation of ice crystals in mixed-phase or cirrus clouds, especially when other effective INPs, such as mineral dust, marine particles, or bioaerosols, are present in lower concentrations or absent. Thus, MPs may be able to substantially affect cloud formation. These findings provide new insights into the potential role of MPs as INPs, highlighting their possible impact on cloud formation and other atmospheric processes.

It is important to note that the reported results represent spatial and temporal averages and that MP concentrations are considerably variable. In certain regions, such as those influenced by higher MP emissions or specific atmospheric conditions, the local contribution of MPs to INP concentrations could be much higher than the reported averages.

Nevertheless, our analysis has some limitations. One of them is the highly uncertain size and shape distribution of emitted MPs. So far, we have reported values only as averages over these size distributions. However, when MP emissions are dominated by smaller (PM2.5) particles, MPs contribute an average of about 9% and can exceed 50% of the total INP number concentration (including mineral dust, marine-sourced aerosol, and MPs) under immersion freezing conditions in the tropics in the MAX scenario. In contrast, when larger particles dominate, the average contribution of MPs for the same conditions is around 4% and the maximum is around 30%, values that are slightly lower than those reported as the average over all size distributions. Under cirrus conditions in the tropical Pacific, the maximum contribution of MPs reaches approximately 10% when smaller particles dominate and about 5% when larger particles are more prevalent, with corresponding average contributions of 2% and 0.1%

in the MAX scenario. Clearly, shifting between size distribution scenarios results in noticeable differences in MP contributions.

A further limitation of our study is the omission of different aging processes, such as exposure to UV irradiation, ozone, aqueous sulfuric acid, aqueous ammonium sulfate, or biofilm coating. Busse et al. (2024) reported that UVB exposure increased the ice nucleation efficiency of PP and PVC but decreased it for LDPE and PET. Similarly, exposure to aqueous ammonium sulfate significantly enhanced the efficiency of LDPE and PVC while reducing it for PP and PET. According to Teska et al. (2024), biofilm coatings on microplastics substantially increase their ice nucleation efficiency, reaching levels comparable to efficient INPs such as bacteria, fungi, and lichen. Additionally, prolonged UV irradiation can fracture airborne particles, forming smaller particles. This fracturing process reduces settling velocity, enhances vertical transport, and may create additional ice nucleation sites on particle surfaces (Seifried et al., 2024). Understanding the interaction of MPs with various environmental factors is therefore critical to assessing their ice nucleation efficiency. This highlights the need for further research.

In our study, we also do not consider the diverse chemistry of MPs, which is a crucial factor that may influence their ice nucleation efficiency in various ways. MPs in the atmosphere consist of a wide range of polymers, each containing varying levels of additives, stabilizers, and anti-aging agents. Depending on the polymer type, the ice nucleation efficiency can remain unchanged, increase, or decrease under certain conditions (Busse et al., 2024; Seifried et al., 2024).

Our modeling analysis focused specifically on road traffic-related MPs as potential INPs. However, the total contribution of MPs could be significantly larger when considering additional sources of MP pollution, such as emissions from industry, consumer products, agriculture, and secondary emissions. For instance, Brahney et al. (2021) estimated the secondary emissions from the ocean to be the main source of MPs to the atmosphere. In addition, particles with higher aspect ratios ($AR > 20$), that is, larger surface areas, such as elongated fibers, or of smaller sizes ($d_{eq} < 0.5$ μm) have a greater transport potential and consequently longer residence times in the atmosphere than those considered in this study. This can potentially increase the INP number concentrations at high altitudes. Additionally, as noted by Seifried et al. (2024), elongated particles contain a larger number of active sites that trigger ice nucleation compared to spherical particles of the same mass, and thus initiate freezing at warmer temperatures. As we have shown, increased hydrophobicity can lead to higher overall MP number concentrations. Nevertheless, the exact scavenging efficiencies of MP particles at the moment of their emission into the atmosphere and during subsequent aging remain uncertain.

Another critical point is the absence of in situ observations of MPs at high altitudes, which limits our ability to validate the obtained MP concentrations. Given this, and the demonstrated possible importance of MPs for ice nucleation, we highlight the necessity of more extensive high-altitude sampling of MPs.

Finally, MP concentrations in the atmosphere could grow significantly in the future due to the nearly threefold projected increase in plastic production by 2060 (OECD, 2022), potentially amplifying the role of MPs in cloud formation and, consequently, in the climate system. This underscores the importance of further research into MPs as INPs and their potential impacts on climate.

Conflict of Interest

The authors declare no conflicts of interest relevant to this study.

Data Availability Statement

The source code of FLEXPART v11 is freely available from Bakels et al. (2024a). The data underlying this study are available from Tatsii, Gasparini, et al. (2024b).

Acknowledgments
We acknowledge support from the University of Vienna's research platform PLENTY (Plastics in the Environment and Society). The model simulations were run on the High-Performance Computing (HPC) system provided by Vienna Scientific Cluster (VSC). Open Access funding provided by Universitat Wien/KEMÖ.

References

Abbasi, S., Rezaei, M., Mina, M., Sameni, A., Oleszczuk, P., Turner, A., & Ritsema, C. (2023). Entrainment and horizontal atmospheric transport of microplastics from soil. *Chemosphere*, *322*, 138150. https://doi.org/10.1016/j.chemosphere.2023.138150

Aeschlimann, M., Li, G., Kanji, Z. A., & Mitrano, D. M. (2022). Potential impacts of atmospheric microplastics and nanoplastics on cloud formation processes. *Nature Geoscience*, *15*(12), 967–975. https://doi.org/10.1038/s41561-022-01051-9

Ahmed, R., Hamid, A. K., Krebsbach, S. A., He, J., & Wang, D. (2022). Critical review of microplastics removal from the environment. *Chemosphere*, *293*, 133557. https://doi.org/10.1016/j.chemosphere.2022.133557

Allen, D., Allen, S., Abbasi, S., Baker, A., Bergmann, M., Brahney, J., et al. (2022). Microplastics and nanoplastics in the marine-atmosphere environment. *Nature Reviews Earth & Environment*, *3*(6), 393–405. https://doi.org/10.1038/s43017-022-00292-x

Allen, S., Allen, D., Phoenix, V., Le Roux, G., Jiménez, P., Simonneau, A., et al. (2019). Atmospheric transport and deposition of microplastics in a remote mountain catchment. *Nature Geoscience*, *12*(5), 339–344. https://doi.org/10.1038/s41561-019-0335-5

Amann, M., Bertok, I., Borken-Kleefeld, J., Cofala, J., Heyes, C., Höglund-Isaksson, L., et al. (2011). Cost-effective control of air quality and greenhouse gases in europe: Modeling and policy applications. *Environmental Modelling & Software*, *26*(12), 1489–1501. https://doi.org/10.1016/j.envsoft.2011.07.012

Bakels, L., Tatsii, D., Tipka, A., Thompson, R., Dütsch, M., Blaschek, M., et al. (2024b). Flexpart version 11: Improved accuracy, efficiency, and flexibility. *EGUsphere*, *2024*, 1–50. https://doi.org/10.5194/egusphere-2024-1713

Bakels, L., Tatsii, D., Tipka, A., Thompson, R., Dütsch, M., Blaschek, M., et al. (2024a). FLEXPART-v11 [Software]. *Zenodo*. https://doi.org/10.5281/zenodo.13748655

Beer, C. G., Hendricks, J., & Righi, M. (2022). A global climatology of ice-nucleating particles under cirrus conditions derived from model simulations with MADE3 in EMAC. *Atmospheric Chemistry and Physics*, *22*(24), 15887–15907. https://doi.org/10.5194/acp-22-15887-2022

Berry, E., & Mace, G. G. (2014). Cloud properties and radiative effects of the Asian summer monsoon derived from a-train data. *Journal of Geophysical Research: Atmospheres*, *119*(15), 9492–9508. https://doi.org/10.1002/2014jd021458

Bolot, M., & Fueglistaler, S. (2021). Tropical water fluxes dominated by deep convection up to near tropopause levels. *Geophysical Research Letters*, *48*(4), e2020GL091471. https://doi.org/10.1029/2020GL091471

Brahney, J., Mahowald, N., Prank, M., Cornwell, G., Klimont, Z., Matsui, H., & Prather, K. A. (2021). Constraining the atmospheric limb of the plastic cycle. *Proceedings of the National Academy of Sciences of the United States of America*, *118*(16), e2020719118. https://doi.org/10.1073/pnas.2020719118

Broeke, H., Hulskotte, J., & Denier van der Gon, H. (2008). *Road traffic tire wear. Emission estimates for diffuse sources, Netherlands emission inventory (Tech. Rep.)*. Netherlands National Water Board – Water Unit.

Bucci, S., Richon, C., & Bakels, L. (2024). Exploring the transport path of oceanic microplastics in the atmosphere. *Environmental Science & Technology*, *58*(32), 14338–14347. https://doi.org/10.1021/acs.est.4c03216

Burghardt, T. E., & Pashkevich, A. (2023). Road markings and microplastics – A critical literature review. *Transportation Research Part D: Transport and Environment*, *119*, 103740. https://doi.org/10.1016/j.trd.2023.103740

Busse, H. L., Ariyasena, D. D., Orris, J., & Freedman, M. A. (2024). Pristine and aged microplastics can nucleate ice through immersion freezing. *ACS ES&T Air*, *1*(12), 1579–1588. https://doi.org/10.1021/acsestair.4c00146

Chatziparaschos, M., Daskalakis, N., Myriokefalitakis, S., Kalivitis, N., Nenes, A., Gonçalves Ageitos, M., et al. (2023). Role of k-feldspar and quartz in global ice nucleation by mineral dust in mixed-phase clouds. *Atmospheric Chemistry and Physics*, *23*(3), 1785–1801. https://doi.org/10.5194/acp-23-1785-2023

Checa-Garcia, R., Balkanski, Y., Albani, S., Bergman, T., Carslaw, K., Cozic, A., et al. (2021). Evaluation of natural aerosols in crescendo earth system models (ESMS): Mineral dust. *Atmospheric Chemistry and Physics*, *21*(13), 10295–10335. https://doi.org/10.5194/acp-21-10295-2021

Chen, J., Wu, Z., Gong, X., Qiu, Y., Chen, S., Zeng, L., & Hu, M. (2024). Anthropogenic dust as a significant source of ice-nucleating particles in the urban environment. *Earth's Future*, *12*(1), e2023EF003738. https://doi.org/10.1029/2023EF003738

Enfrin, M., Myszka, R., & Giustozzi, F. (2022). Paving roads with recycled plastics: Microplastic pollution or eco-friendly solution? *Journal of Hazardous Materials*, *437*, 129334. https://doi.org/10.1016/j.jhazmat.2022.129334

Evangeliou, N., Grythe, H., Klimont, Z., Heyes, C., Eckhardt, S., Lopez-Aparicio, S., & Stohl, A. (2020). Atmospheric transport is a major pathway of microplastics to remote regions. *Nature Communications*, *11*, 1–11. https://doi.org/10.1038/s41467-020-17201-9

Evangelou, I., Tatsii, D., Bucci, S., & Stohl, A. (2024). Atmospheric resuspension of microplastics from bare soil regions. *Environmental Science & Technology*, *58*(22), 9741–9749. https://doi.org/10.1021/acs.est.4c01252

Froyd, K. D., Yu, P., Schill, G. P., Brock, C. A., Kupc, A., Williamson, C. J., et al. (2022). Dominant role of mineral dust in cirrus cloud formation revealed by global-scale measurements. *Nature Geoscience*, *15*(3), 177–183. https://doi.org/10.1038/s41561-022-00901-w

Ganguly, M., & Ariya, P. A. (2019). Ice nucleation of model nanoplastics and microplastics: A novel synthetic protocol and the influence of particle capping at diverse atmospheric environments. *ACS Earth and Space Chemistry*, *3*(9), 1729–1739. https://doi.org/10.1021/acsearthspacechem.9b00132

Gasparini, B., & Lohmann, U. (2016). Why cirrus cloud seeding cannot substantially cool the planet. *Journal of Geophysical Research: Atmospheres*, *121*(9), 4877–4893. https://doi.org/10.1002/2015JD024666

Gasparini, B., Sullivan, S. C., Sokol, A. B., Kärcher, B., Jensen, E., & Hartmann, D. L. (2023). Opinion: Tropical cirrus – From micro-scale processes to climate-scale impacts. *Atmospheric Chemistry and Physics*, *23*(24), 15413–15444. https://doi.org/10.5194/acp-23-15413-2023

Grigoratos, T., & Martini, G. (2014). *Non-exhaust traffic related emissions - brake and tyre wear pm – literature review*. Publications Office of the European Union. https://doi.org/10.2790/21481

Groot Zwaaftink, C. D., Grythe, H., Skov, H., & Stohl, A. (2016). Substantial contribution of northern high-latitude sources to mineral dust in the arctic. *Journal of Geophysical Research: Atmospheres*, *121*(22), 13678–13697. https://doi.org/10.1002/2016JD025482

Hale, R. C., Seeley, M. E., La Guardia, M. J., Mai, L., & Zeng, E. Y. (2020). A global perspective on microplastics. *Journal of Geophysical Research: Oceans*, *125*(1), e2018JC014719. https://doi.org/10.1029/2018JC014719

Harrison, R. M., Jones, A. M., Gietl, J., Yin, J., & Green, D. C. (2012). Estimation of the contributions of brake dust, tire wear, and resuspension to nonexhaust traffic particles derived from atmospheric measurements. *Environmental Science & Technology*, *46*(12), 6523–6529. https://doi.org/10.1021/es300894r

Hartmann, D. L., & Berry, S. E. (2017). The balanced radiative effect of tropical anvil clouds. *Journal of Geophysical Research: Atmospheres*, *122*(9), 5003–5020. https://doi.org/10.1002/2017JD026460

Hawker, R. E., Miltenberger, A. K., Johnson, J. S., Wilkinson, J. M., Hill, A. A., Shipway, B. J., et al. (2021). Model emulation to understand the joint effects of ice-nucleating particles and secondary ice production on deep convective anvil cirrus. *Atmospheric Chemistry and Physics*, *21*(23), 17315–17343. https://doi.org/10.5194/acp-21-17315-2021

Hendricks, J., Kärcher, B., & Lohmann, U. (2011). Effects of ice nuclei on cirrus clouds in a global climate model. *Journal of Geophysical Research*, *116*(D18), D18206. https://doi.org/10.1029/2010JD015302

Herbert, R. J., Sanchez-Marroquin, A., Grosvenor, D. P., Pringle, K. J., Arnold, S. R., Murray, B. J., & Carslaw, K. S. (2025). Gaps in our understanding of ice-nucleating particle sources exposed by global simulation of the UK Earth System Model. *Atmospheric Chemistry and Physics*, *25*(1), 291–325. https://doi.org/10.5194/acp-25-291-2025

Hersbach, H., Bell, B., Berrisford, P., Hirahara, S., Horányi, A., Muñoz-Sabater, J., et al. (2020). The era5 global reanalysis. *Quarterly Journal of the Royal Meteorological Society*, *146*(730), 1999–2049. https://doi.org/10.1002/qj.3803

Hussein, T., Johansson, C., Karlsson, H., & Hansson, H.-C. (2008). Factors affecting non-tailpipe aerosol particle emissions from paved roads: On-road measurements in Stockholm, Sweden. *Atmospheric Environment*, *42*(4), 688–702. https://doi.org/10.1016/j.atmosenv.2007.09.064

Järlskog, I., Jaramillo-Vogel, D., Rausch, J., Perseguers, S., Gustafsson, M., Strömvall, A.-M., & Andersson-Sköld, Y. (2022). Differentiating and quantifying carbonaceous (tire, bitumen, and road marking wear) and non-carbonaceous (metals, minerals, and glass beads) non-exhaust particles in road dust samples from a traffic environment. *Water, Air, & Soil Pollution*, *233*(9), 375. https://doi.org/10.1007/s11270-022-05847-8

Jensen, E. J., Diskin, G., Lawson, R. P., Lance, S., Bui, T. P., Hlavka, D., et al. (2013). Ice nucleation and dehydration in the tropical tropopause layer. *Proceedings of the National Academy of Sciences of the United States of America*, *110*(6), 2041–2046. https://doi.org/10.1073/pnas.1217104110

Jensen, E. J., Pfister, L., Jordan, D. E., Bui, T. V., Ueyama, R., Singh, H. B., et al. (2017). The NASA airborne tropical tropopause experiment: High-altitude aircraft measurements in the tropical western pacific. *Bulletin of the American Meteorological Society*, *98*(1), 129–143. https://doi.org/10.1175/BAMS-D-14-00263.1

Jiang, H., Bu, J., Bian, K., Su, J., Wang, Z., Sun, H., et al. (2023). Surface change of microplastics in aquatic environment and the removal by froth flotation assisted with cationic and anionic surfactants. *Water Research*, *233*, 119794. https://doi.org/10.1016/j.watres.2023.119794

Kanji, Z. A., Ladino, L. A., Wex, H., Boose, Y., Burkert-Kohn, M., Cziczo, D. J., & Krämer, M. (2017). Overview of ice nucleating particles. *Meteorological Monographs*, *58*, 1.1–1.33. https://doi.org/10.1175/AMSMONOGRAPHS-D-16-0006.1

Kau, D., Materić, D., Holzinger, R., Baumann-Stanzer, K., Schauer, G., & Kasper-Giebl, A. (2024). Fine micro- and nanoplastics concentrations in particulate matter samples from the high alpine site Sonnblick, Austria. *Chemosphere*, *352*, 141410. https://doi.org/10.1016/j.chemosphere.2024.141410

Kole, P. J., Löhr, A. J., Van Belleghem, F. G. A. J., & Ragas, A. M. J. (2017). Wear and tear of tyres: A stealthy source of microplastics in the environment. *International Journal of Environmental Research and Public Health*, *14*(10), 1265. https://doi.org/10.3390/ijerph14101265

Korolev, A., McFarquhar, G., Field, P. R., Franklin, C., Lawson, P., Wang, Z., et al. (2017). Mixed-phase clouds: Progress and challenges. *Meteorological Monographs*, *58*(5), 1–5.50. https://doi.org/10.1175/AMSMONOGRAPHS-D-17-0001.1

Kovochich, M., Parker, J. A., Oh, S. C., Lee, J. P., Wagner, S., Reemtsma, T., & Unice, K. M. (2021). Characterization of individual tire and road wear particles in environmental road dust, tunnel dust, and sediment. *Environmental Science and Technology Letters*, *8*(12), 1057–1064. https://doi.org/10.1021/acs.estlett.1c00811

Kreider, M. L., Panko, J. M., McAtee, B. L., Sweet, L. I., & Finley, B. L. (2010). Physical and chemical characterization of tire-related particles: Comparison of particles generated using different methodologies. *Science of the Total Environment*, *408*(3), 652–659. https://doi.org/10.1016/j.scitotenv.2009.10.016

Kuebbeler, M., Lohmann, U., Hendricks, J., & Kärcher, B. (2014). Dust ice nuclei effects on cirrus clouds. *Atmospheric Chemistry and Physics*, *14*(6), 3027–3046. https://doi.org/10.5194/acp-14-3027-2014

Matus, A. V., & L'Ecuyer, T. S. (2017). The role of cloud phase in earth's radiation budget. *Journal of Geophysical Research: Atmospheres*, *122*(5), 2559–2578. https://doi.org/10.1002/2016JD025951

Meijer, J. R., Huijbregts, M. A. J., Schotten, K. C. G. J., & Schipper, A. M. (2018). Global patterns of current and future road infrastructure. *Environmental Research Letters*, *13*(6), 064006. https://doi.org/10.1088/1748-9326/aabd42

Morioka, T., Tanaka, S., Yamada, Y., Yukioka, S., & Aiba, F. (2023). Quantification of microplastic by particle size down to 1.1 m in surface road dust in an urban city, Japan. *Environmental Pollution*, *334*, 122198. https://doi.org/10.1016/j.envpol.2023.122198

Murray, B. J., Carslaw, K. S., & Field, P. R. (2021). Opinion: Cloud-phase climate feedback and the importance of ice-nucleating particles. *Atmospheric Chemistry and Physics*, *21*(2), 665–679. https://doi.org/10.5194/acp-21-665-2021

Murray, B. J., O'Sullivan, D., Atkinson, J. D., & Webb, M. E. (2012). Ice nucleation by particles immersed in supercooled cloud droplets. *Chemical Society Reviews*, *41*(19), 6519–6554. https://doi.org/10.1039/C2CS35200A

Myszka, R., Enfrin, M., & Giustozzi, F. (2023). Microplastics in road dust: A practical guide for identification and characterisation. *Chemosphere*, *315*, 137757. https://doi.org/10.1016/j.chemosphere.2023.137757

OECD. (2022). Global plastics outlook. https://doi.org/10.1787/aa1edf33-en

Pyshyev, S., Gunka, V., Grytsenko, Y., & Bratychak, M. (2016). Polymer modified bitumen: Review. *Chemistry and Chemical Technology*, *10*(4), 631–636. https://doi.org/10.23939/chcht10.04si.631

Sassen, K., Wang, Z., & Liu, D. (2008). Global distribution of cirrus clouds from cloudsat/cloud-aerosol lidar and infrared pathfinder satellite observations (CALIPSO) measurements. *Journal of Geophysical Research*, *113*(D8), D00A12. https://doi.org/10.1029/2008JD009972

Seifried, T. M., Nikkho, S., Morales Murillo, A., Andrew, L. J., Grant, E. R., & Bertram, A. K. (2024). Microplastic particles contain ice nucleation sites that can be inhibited by atmospheric aging. *Environmental Science & Technology*, *58*(35), 15711–15721. https://doi.org/10.1021/acs.est.4c02639

Seinfeld, J. H., Bretherton, C., Carslaw, K. S., Coe, H., DeMott, P. J., Dunlea, E. J., et al. (2016). Improving our fundamental understanding of the role of aerosolcloud interactions in the climate system. *Proceedings of the National Academy of Sciences of the United States of America*, *113*(21), 5781–5790. https://doi.org/10.1073/pnas.1514043113

Snilsberg, B., Myran, T., Uthus, N., & Aurstad, J. (2008). Evaluation of different laboratory methods for simulation of pavement wear and road dust generation. *Road Materials and Pavement Design*, *9*(sup1), 287–304. https://doi.org/10.1080/14680629.2008.9690170

Sommer, F., Dietze, V., Baum, A., Sauer, J., Gilge, S., Maschowski, C., & Gieré, R. (2018). Tire abrasion as a major source of microplastics in the environment. *Aerosol and Air Quality Research*, *18*(8), 2014–2028. https://doi.org/10.4209/aaqr.2018.03.0099

Tan, I., Storelvmo, T., & Zelinka, M. D. (2016). Observational constraints on mixed-phase clouds imply higher climate sensitivity. *Science*, *352*(6282), 224–227. https://doi.org/10.1126/science.aad5300

Tatsii, D., Bucci, S., Bhowmick, T., Guettler, J., Bakels, L., Bagheri, G., & Stohl, A. (2024). Shape matters: Long-range transport of microplastic fibers in the atmosphere. *Environmental Science & Technology*, *58*(1), 671–682. https://doi.org/10.1021/acs.est.3c08209

Tatsii, D., Gasparini, B., Evangelou, I., Bucci, S., & Stohl, A. (2024). Data underlying the study 'Do microplastics contribute to the total number concentration of ice nucleating particles? [Dataset]. *Zenodo*. https://doi.org/10.5281/zenodo.14548491

Tegen, I., Neubauer, D., Ferrachat, S., Siegenthaler-Le Drian, C., Bey, I., Schutgens, N., et al. (2019). The global aerosol–climate model ECHAM6.3–HAM2.3 – Part 1: Aerosol evaluation. *Geoscientific Model Development*, *12*(4), 1643–1677. https://doi.org/10.5194/gmd-12-1643-2019

Teska, C. J., Dieser, M., & Foreman, C. M. (2024). Clothing textiles as carriers of biological ice nucleation active particles. *Environmental Science & Technology*, *58*(14), 6305–6312. https://doi.org/10.1021/acs.est.3c09600

Thomson, D. S., Schein, M. E., & Murphy, D. M. (2000). Particle analysis by laser mass spectrometry wb-57f instrument overview. *Aerosol Science & Technology*, *33*(1–2), 153–169. https://doi.org/10.1080/027868200410903

Vergara-Temprado, J., Miltenberger, A. K., Furtado, K., Grosvenor, D. P., Shipway, B. J., Hill, A. A., et al. (2018). Strong control of southern ocean cloud reflectivity by ice-nucleating particles. *Proceedings of the National Academy of Sciences of the United States of America*, *115*(11), 2687–2692. https://doi.org/10.1073/pnas.1721627115

Vogelsang, C., Lusher, A., Dadkhah, M., Sundvor, I., Umar, M., Ranneklev, S., et al. (2018). Microplastics in road dust - characteristics, pathways and measures.

Wang, Y., Okochi, H., Tani, Y., Hayami, H., Minami, Y., Katsumi, N., et al. (2023). Airborne hydrophilic microplastics in cloud water at high altitudes and their role in cloud formation. *Environmental Chemistry Letters*, *21*(6), 3055–3062. https://doi.org/10.1007/s10311-023-01626-x

Wilkinson, T., Järlskog, I., de Lima, J. A., Gustafsson, M., Mattsson, K., Andersson Sköld, Y., & Hassellöv, M. (2023). Shades of grey—Tire characteristics and road surface influence tire and road wear particle (TRWP) abundance and physicochemical properties. *Frontiers in Environmental Science*, *11*. https://doi.org/10.3389/fenvs.2023.1258922

Wofsy, S., Afshar, S., Allen, H., Apel, E., Asher, E., Barletta, B., et al. (2018). *Atom: Merged atmospheric chemistry, trace gases, and aerosols*. ORNL Distributed Active Archive Center. https://doi.org/10.3334/ORNLDAAC/1581

Xu, X., Li, T., Zhen, J., Jiang, Y., Nie, X., Wang, Y., et al. (2024). Characterization of microplastics in clouds over eastern China. *Environmental Science and Technology Letters*, *11*(1), 16–22. https://doi.org/10.1021/acs.estlett.3c00729